The Filtering Approach to Solvent Peak Suppression in MRS: A Critical Review

Alain Coron,*,1 Leentje Vanhamme,†,2 Jean-Pierre Antoine,‡,3 Paul Van Hecke,§,4 and Sabine Van Huffel†,5

*Department of Applied Physics, Delft University of Technology, P.O. Box 5046, 2600 GA Delft, The Netherlands; †Department of Electrical Engineering (ESAT), Katholieke Universiteit Leuven, Kasteelpark Arenberg 10, 3001 Leuven, Belgium; ‡Institut de Physique Théorique, Université Catholique de Louvain, 2 chemin du Cyclotron, B-1348 Louvain-la-Neuve, Belgium; and §Biomedical NMR Unit, Katholieke Universiteit Leuven, Gasthuisberg, 3000 Leuven, Belgium

Suppressing the solvent peak is important in many applications of biomedical NMR spectroscopy in order to quantify the metabolites with a great accuracy. Among the postprocessing methods proposed in the literature, many deal with the concept of filtering. However, several proposals lack a theoretical perspective and some have not been explicitly applied to quantification problems. The present article is intended to bridge this gap: five methods are analyzed from a theoretical perspective. Subsequently the different methods are applied to the same set of data, and then the latter are quantified using the model fitting method AMARES. With our set, the scheme proposed by T. Sundin *et al.* (*J. Magn. Reson.* 139(2), 189–204 (1999)) proved to be the most reliable method. © 2001 Academic Press

Key Words: peak suppression; quantitation; filter; time-frequency analysis.

1. INTRODUCTION

In biomedical applications of proton NMR spectroscopy, the large solvent water resonance must be suppressed in order to allow an adequate quantitation of the solute. However, as one usually intends to quantify metabolites, suppressing the solvent peak should not alter them.

Many methods have been proposed in the literature and they can be classified in two groups: on the one hand, the pulse sequence methods and hardware methods, on the other hand, the postprocessing methods (*1*). The two groups should be used in conjunction for better results.

Most of the proposed postprocessing methods rely implicitly or explicitly on the signal processing concept of filtering. However, several proposals lack a theoretical perspective and some have not been explicitly applied to quantification problems.

The aim of the article is to alleviate these shortcomings by:

• making the connection between some of the methods from a theoretical point of view;

• comparing the accuracy of the final parameter estimates obtained by quantifying the signals processed by the different methods.

The methods we have chosen are:

• a Gabor transform based method (*2*), which is a valuable alternative to the wavelet transform based method (*3–5*);
• the method of Marion *et al.* (*6*);
• the method of Sodano and Delepierre (*7*);
• the Cross method (*8*);
• the Finite Impulse Response (FIR) filter based method developed by Sundin *et al.* (*9*).

These have been chosen because they are based on filtering and they provide variations on the "filtering scheme."

2. FILTERING AN NMR FID

In this Section, we study the different solvent peak suppression methods from a theoretical point of view. In Section 2.1 we explain the common feature of all compared methods, i.e., the extraction of the solvent signal using a filter. We then discuss the inherent difficulties associated with the use of a filter. In Sections 2.2 to 2.6 we describe the different implementation aspects of each method in detail and examine the consequences of the solvent removal step on the quantification procedure. Finally, in Section 2.7 the main characteristics of the filtering methods are summarized.

2.1. The Filtering Method and Its Limitations

The general form of a water or metabolite peak of an FID signal is $S(t) = A(t)e^{i(\omega_0 t + \phi)}U(t)$ where:

• the pulsation and the phase at the time origin of the peak are $\omega_0 \in \mathbb{R}$ and $\phi \in \mathbb{R}$;

¹ E-mail: coro@si.tn.tudelft.nl.
² E-mail: Leentje.Vanhamme@esat.kuleuven.ac.be.
³ To whom correspondence should be addressed. E-mail: antoine@fyma.ucl.ac.be.
⁴ E-mail: Paul.VanHecke@med.kuleuven.ac.be.
⁵ E-mail: Sabine.VanHuffel@esat.kuleuven.ac.be.

- $A(t)$, the amplitude of the signal, is of finite energy, real, positive, and regular on $\mathbb{R}$. The exact definition of regular is provided in Appendix B. For an FID, $A(t)$ has a maximum around $t = 0$ and decreases when t increases. The exact form of the peaks is usually unknown. However, the amplitude of the metabolite peaks will sometimes explicitly be modeled with a damped exponential.
- $U(t)$ is the Heaviside step function:

$$U(t) = \begin{cases} 0 & \text{if } t < 0, \\ 1 & \text{if } t \geq 0 \end{cases}$$

As soon as $A(0) \neq 0$, $S(t)$ is discontinuous at $t = 0$. So the Fourier transform $\hat{S}(\omega)$ of $S(t)$ decays slowly at high frequency, leading to a large peak tail (see Appendix A for some useful properties of the Fourier transform $\hat{S}$ of the signal S).

In the sequel, we explain how the water peak can be suppressed using a generalized filtering framework.

Once and for all, we assume that T_1 and T_2 are two real constants with $-\infty \leq T_1 < T_2 \leq +\infty$ and that the support of the function f is $[T_1, T_2]$, i.e., $f(t) = 0$ if $t \notin [T_1, T_2]$. The energy of f is supposed to be finite.

By * and $\bar{f}$, we denote the complex conjugate and the function $\bar{f}(\tau) = f^*(-\tau)$ respectively. We also define the family of functions $f_{t,\omega}(\tau) = f(\tau - t)e^{i\omega(\tau - t)}$ with $(t, \omega) \in \mathbb{R}^2$. Each element of this family is a frequency and time translated version of the reference function f.

The following function,

$$G_{\bar{f},S}(t, \omega) = \langle (\bar{f})_{t,\omega}, S \rangle$$
$$= \int_{\mathbb{R}} (\bar{f}(\tau - t)e^{i\omega(\tau - t)})^* S(\tau)\, d\tau \qquad [1]$$

can be interpreted as a weighted sum of $(\bar{f})_{t,\omega}$ and S. It defines the Gabor transform of S with a window $\bar{f}$ and is a generalization of the filtering notion because

$$G_{\bar{f},S}(t, 0) = f * S(t). \qquad [2]$$

According to Appendix B, an approximate expression of $G_{\bar{f},S}(t, \omega)$ under the assumption that $A(\tau)$ varies slowly on $[-T_2 + t, -T_1 + t]$ is

$$G_{\bar{f},S}(t, \omega) = e^{i(\omega_0(t-l)+\phi+\omega l)}(A(t-l)\widehat{\bar{f}_{-l,0}}(\omega_0 - \omega) + C_1(t, \omega))$$
$$\qquad [3]$$
$$= S(t-l)e^{i\omega l}\hat{f}(\omega_0 - \omega) + e^{i(\omega_0(t-l)+\phi+\omega l)}C_1(t, \omega).$$
$$\qquad [4]$$

In the previous equations,

- l is the point where f is maximum or the average location. In the latter case,

$$l = \frac{\int_{\mathbb{R}} t|f(t)|^2\, dt}{\int_{\mathbb{R}} |f(t)|^2\, dt}.$$

- $C_1(t, \omega)$ is an error term that can be bounded.

Then, under the assumption that $A(\tau)$ varies slowly on $[-T_2 + t, -T_1 + t]$, which means that $A^{(1)}(\tau)$, the first derivative of $A(\tau)$, is very small on this interval, $G_{\bar{f},S}(t, \omega_0)$ and the filtering method lead to good approximations of S up to a correction term. So with $|\hat{f}(0)| \approx 1$, one can extract S from these transformations, even if the exact shape of $A(t)$ is unknown:

$$S(t - l) \approx \frac{G_{\bar{f},S}(t, \omega_0)}{e^{i\omega_0 l}\hat{f}(0)}. \qquad [5]$$

In general, one extracts or suppresses one component S_0 among the sum S of many others. Let us now write $S(t)$ as

$$S(t) = \sum_{k=0}^{m} S_k(t) = \sum_{k=0}^{m} A_k(t)e^{i(\omega_k t + \phi_k)}U(t),$$

and by linearity of $G_{\bar{f},S}$,

$$G_{\bar{f},S}(t, \omega) = \sum_{k=0}^{m} S_k(t-l)e^{i\omega_k l}\hat{f}(\omega_k - \omega) + \epsilon(t, \omega). \qquad [6]$$

With $\omega = \omega_0$ the component $S_0(t)$ can be well extracted or suppressed if the bandstop or bandpass of f is sharp enough.

However, because of the discontinuity of the FID at $t = 0$, this approximation is valid only for $t < T_1$ or $t \geq T_2$, that is, outside of the transients.

From another point of view, and according to the continuity property of a filtered signal (see Appendix A), $G_{\bar{f},S}(t, \omega)$ is continuous at each point t on $\mathbb{R}$, although we intend to extract/suppress from S one and only one component S_k that is discontinuous at $t = 0$. This is the main difficulty.

So the question is: Is it possible to recover S_k and in particular points around its discontinuity with a filter based technique? From an accurate quantitative perspective, properly getting those first points is essential because the power of the metabolites components is maximum there.

Before studying the solution proposed by the different authors, let us point out an exact result concerning the metabolite represented by modulated damped exponentials (9). Defining

$$S(t) = \sum_{k=1}^{m} S_k(t) = \sum_{k=1}^{m} A_k e^{-d_k t} e^{i(\omega_k t + \phi_k)}U(t),$$

CORON ET AL.

its transform $G_{\bar{f},S}$ is

$$G_{\bar{f},S}(t,\omega) = \sum_{k=1}^{m} A_k e^{-d_k t} e^{i(\omega_k t + \phi_k)}$$

$$\times \int_{T_1}^{T_2} f(u) e^{d_k u - i(\omega_k - \omega)u} U(t-u)\,du.$$

If $t \geq T_2$ the shape of the metabolite signals remains unchanged after filtering,

$$G_{\bar{f},S}(t,\omega) = \sum_{k=1}^{m} S_k(t) F_{\bar{f},k}(\omega) \qquad [7]$$

up to some weighting factors:

$$F_{\bar{f},k}(\omega) = \int_{\mathbb{R}} f(u) e^{d_k u - i(\omega_k - \omega)u}\,du. \qquad [8]$$

Compare Eq. [6] with [7]; If $d_k = 0$, $F_{\bar{f},k}(\omega) = \hat{f}(\omega_k - \omega)$.

Now, we will examine the five solutions mentioned in the introduction. We will explain their specific implementation details and their effect on the actual estimation of the parameters of the metabolites of interest. The methods mainly differ in the exact choice of filter and in the treatment of the datapoints for $t < T_2$.

We consider that the analyzed signal $S(t)$ is the sum of a solvent peak $S_0(t)$ and m metabolite peaks $S_k(t)$ ($k \in \{1, \ldots, m\}$), modeled by damped exponentials

$$S(t) = \sum_{k=0}^{m} S_k(t) \qquad [9]$$

$$= \left(A_0(t) e^{i(\omega_0 t + \phi_0)} + \sum_{k=1}^{m} A_k e^{-d_k t} e^{i(\omega_k t + \phi_k)} \right) U(t) \quad [10]$$

with A_0 a regular real and positive function of finite energy, $A_k \in \mathbb{R}^+$, $(d_k, \omega_k, \phi_k) \in \mathbb{R}^+ \times \mathbb{R}^2$ for $k \in \{1, \ldots, m\}$.

2.2. Gabor Solution

As mentioned earlier, Eq. [1] is the definition of the Gabor transform of S. This transformation has many interesting properties (10) and is closely related to the wavelet transform. The wavelet transform was applied more than ten years ago to the solvent suppression problem (4, 5) and later to the dynamical phase correction problem (3).

However from a spectroscopist perspective, the Gabor transform is more natural than the wavelet transform for solving the problems mentioned above. In fact, spectroscopists prefer a transform that is covariant under frequency translation (the Gabor transform) to a transform that is covariant under dilation (the wavelet transform) (2). In other words, if S_1 is a frequency shifted version of S,

$$S_1(t) = e^{i\zeta_0 t} S(t)$$

with $\zeta_0 \in \mathbb{R}$, then the covariance under frequency translation property of the Gabor transform implies that

$$G_{\bar{f},S_1}(t,\omega) = G_{\bar{f},S}(t, \omega - \zeta_0).$$

This property is most welcome in the context of NMR spectroscopy, since frequency translation is very common. Unfortunately, the previous relation does not hold with the wavelet transform, except for the trivial case $\zeta_0 = 0$. Here we focus on the Gabor transform only.

With this method, one chooses a lowpass analyzing window $\bar{f}$ with finite support. Usually, it is a truncated Gaussian or a Hamming window, so it is real and centered around the origin ($l = 0$). The exact window type and width are chosen by the user and not automatically. Then a convergence algorithm will find the estimated position $\dot{\omega}_0$ of the solvent peak in the spectrum, extract it, and remove it from the signal. The last filtering steps of the algorithm are summarized in Fig. 1.
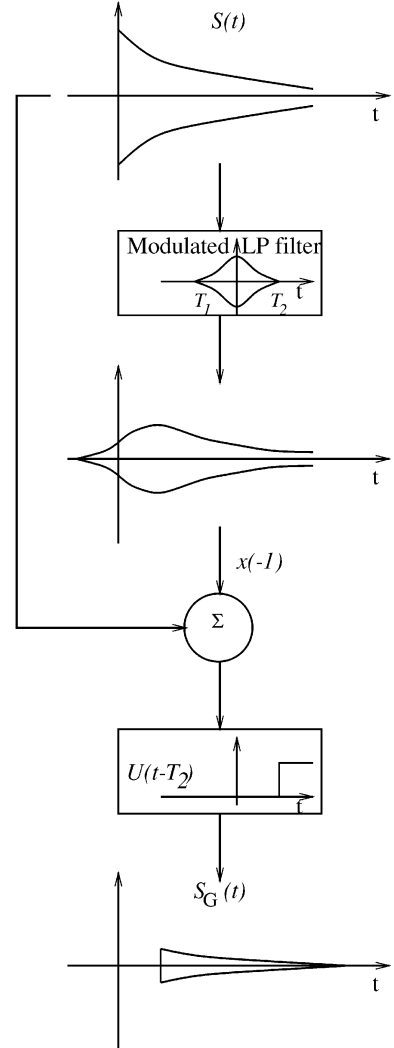

FIG. 1. Schematic representation of the Gabor Method.

Using Eqs. [6], [7], and [10] the signal with the solvent peak suppressed can be approximated by

$$S_G(t) \approx \left(S_0(t)(1 - \hat{f}(\omega_0 - \dot{\omega}_0)) + \sum_{k=1}^{m} S_k(t)(1 - F_{\bar{f},k}(\dot{\omega}_0)) \right)$$
$$\times U(t - T_2). \qquad [11]$$

As no special treatment is provided in (3) for points before T_2, we set them to zero, by multiplying the signal by $U(t - T_2)$. Shifting the origin by posing $\tau = t - T_2$, we get

$$S_G(\tau) \approx \left(S_0(\tau + T_2)(1 - \hat{f}(\omega_0 - \dot{\omega}_0)) + \sum_{k=1}^{m} A_k e^{-d_k T_2} \right.$$
$$\left. \times (1 - F_{\bar{f},k}(\dot{\omega}_0)) e^{-d_k \tau} e^{i(\omega_k \tau + \phi_k + \omega_k T_2)} \right) U(\tau). \quad [12]$$

If $\hat{f}(\omega_0 - \dot{\omega}_0) = 1$ the solvent and its tail are suppressed. The signal is a sum of modulated damped exponentials whose parameters can be estimated using any of the standard estimation methods (e.g., black-box methods such as LPSVD (11) and HSVD (12), interactive methods such as VARPRO (13) and AMARES (14)).

In the sequel, $A'_k, d'_k, \omega'_k, \phi'_k$ denote the estimated parameters of S_G. In order to get a good estimation of the parameters of the original metabolite peaks, and avoid bias, these raw parameters have to be corrected. We propose new estimates that will be denoted by $\dot{A}_k, \dot{d}_k, \dot{\omega}_k, \dot{\phi}_k$:

$$\dot{A}_k = A'_k \frac{e^{d'_k T_2}}{|(1 - F_{\bar{f},k}(\dot{\omega}_0))|} \qquad [13]$$

$$\dot{d}_k = d'_k \qquad [14]$$

$$\dot{\omega}_k = \omega'_k \qquad [15]$$

$$\dot{\phi}_k = \phi'_k - \omega'_k T_2 - \arg(1 - F_{\bar{f},k}(\dot{\omega}_0)). \qquad [16]$$

Note that only the amplitude and the phase have to be corrected.

2.3. The Extrapolation Method of Marion et al.

With this method (6), the frequency of the solvent peak is supposed to be 0. With complex signals, the solvent peak may be shifted to zero by modulation. The signal is filtered with a finite length lowpass filter like a sine-bell or truncated Gaussian function of length $2T_2$ centered on the origin. Its exact shape is chosen by the user. So we get $G_{\bar{f},S}(t, 0)$. Points of $G_{\bar{f},S}(t, 0)$ whose abscissa is smaller than T_2 are not removed, but are replaced by linear extrapolation of the points $G_{\bar{f},S}(T_2, 0)$ and $G_{\bar{f},S}(T_2 + M, 0)$, $(M \in \mathbb{R}^+)$:

$$S'_M(t) = G_{\bar{f},S}(T_2, 0) + \frac{t - T_2}{M}$$
$$\times (G_{\bar{f},S}(T_2 + M, 0) - G_{\bar{f},S}(T_2, 0)). \qquad [17]$$

In the original publication, the signal is supposed to be discrete and because of the circular convolution, one extrapolates also the last T_2 points. In the sequel of this section, we omit the latter interpolation. A schematic diagram of the method is presented in Fig. 2. The solvent peak extracted by Marion et al. is continuous but in general not differentiable at $t = T_2$. Finally, this
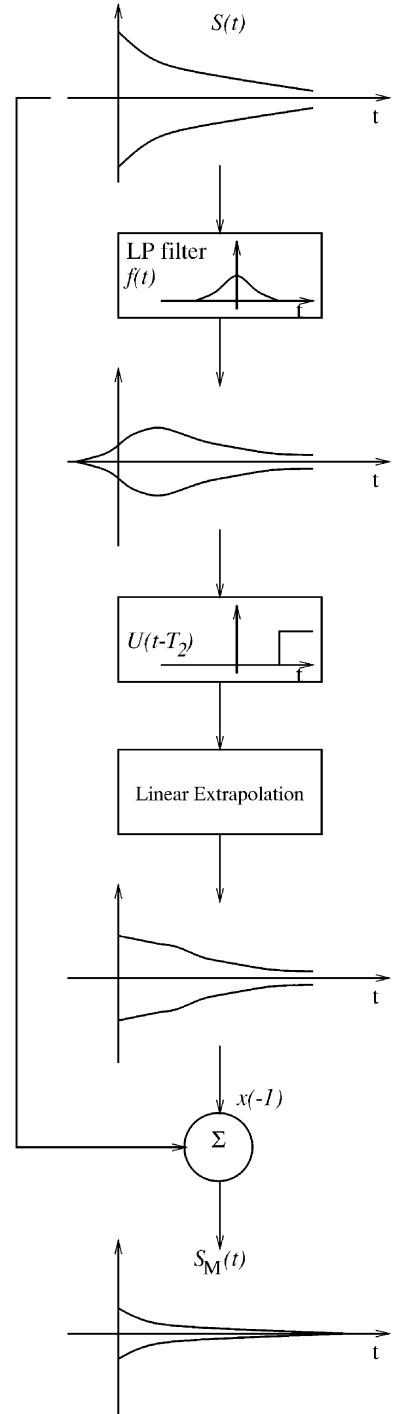

FIG. 2. Schematic representation of the Marion method.

signal is subtracted from the original signal to obtain the solvent suppressed signal $S_M(t)$.

If $t \geq T_2$, an approximation of the solvent suppressed signal is almost the same as Eq. [11],

$$S_M(t) \approx S_0(t)(1 - \hat{f}(0)) + \sum_{k=1}^{m} S_k(t)(1 - F_{\bar{f},k}(0)), \quad [18]$$

and if $t \in [0, T_2)$,

$$S_M(t) \approx S_0(t) - \hat{f}(0)$$
$$\times \left(S_0(T_2) + \frac{T_2 - t}{M}(S_0(T_2) - S_0(T_2 + M)) \right)$$
$$+ \sum_{k=1}^{m} S_k(t)\left(1 - e^{-d_k(T_2-t)}e^{i\omega_k(T_2-t)}F_{\bar{f},k}(0) \right.$$
$$\left. \times \left(1 + \frac{T_2 - t}{M}(1 - e^{-d_k M}e^{i\omega_k M}) \right) \right). \quad [19]$$

So the solvent line will be well suppressed if the linear approximation is valid. The first time points of the metabolites are conserved but might be distorted if $F_{\bar{f},k}(0) \neq 0$. This distortion is time and frequency dependent.

Now if S_M is quantified, it is very difficult to take into account the modified first points. If the estimated parameters of S_M are A_k', d_k', ω_k', and ϕ_k', we propose to estimate, as before, the real parameters with the corrections

$$\dot{A}_k = \frac{A_k'}{|1 - F_{\bar{f},k}(0)|} \quad [20]$$

$$\dot{d}_k = d_k' \quad [21]$$

$$\dot{\omega}_k = \omega_k' \quad [22]$$

$$\dot{\phi}_k = \phi_k' - \arg(1 - F_{\bar{f},k}(0)). \quad [23]$$

2.4. Sodano and Delepierre Solution

The method proposed by Sodano and Delepierre (7) is based on the assumption that the solvent peak S_0 is slowly varying for $t \geq 0$ and differentiable on $\mathbb{R}^*$ with $|\frac{dS_0}{dt}(t)|$ small. As a consequence, the solvent peak $S_0(t)$ centered around $\omega_0 = 0$ is well approximated by $G_{\bar{f},S}(t + T_2, 0)$ $(t \geq 0)$. $f(t)$ is a finite length lowpass filter chosen by the user, whose support is $[-T_2, T_2]$ symmetrical. Then this approximation is subtracted from the original signal (see Fig. 3). According to Eqs. [4], [7], and [10], the signal with the solvent peak suppressed is

$$S_{So}(t) \approx \left(S_0(t) - S_0(t + T_2)\hat{f}(0) \right.$$
$$\left. + \sum_{k=1}^{m} S_k(t)\left(1 - e^{-d_k T_2}e^{i\omega_k T_2}F_{\bar{f},k}(0) \right) \right)U(t). \quad [24]$$
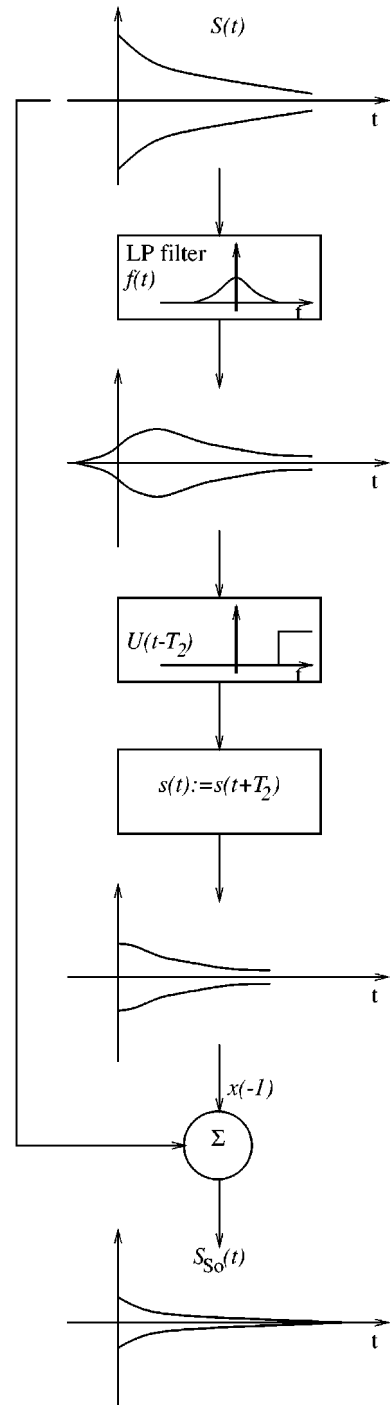

FIG. 3. Schematic representation of the Sodano and Delepierre method.

The discontinuity at $t = 0$ is preserved and the tail of the peak is removed. According to Eq. [24] suitable corrections should be applied on the estimated peak parameters A_k', d_k', ω_k', and ϕ_k' of $S_{So}(t)$. We propose again

$$\dot{A}_k = \frac{A_k'}{|1 - e^{-d_k' T_2}e^{i\omega_k' T_2}F_{\bar{f},k}(0)|} \quad [25]$$

$$\dot{d}_k = d'_k \qquad [26]$$

$$\dot{\omega}_k = \omega'_k \qquad [27]$$

$$\dot{\phi}_k = \phi'_k - \arg(1 - e^{-d'_k T_2} e^{i\omega'_k T_2} F_{\bar{f},k}(0)). \qquad [28]$$

2.5. Cross's Solution

We suppose the solvent peak to be at zero Hertz. If it is not, one modulates the complex signal to shift the solvent peak to zero. In that case, after suppressing the water peak, an extra modulation step will move the spectrum and the metabolite peaks back to their original position.

The signal, with solvent peak at zero frequency, is filtered twice, once backward and then forward with a real causal ($T_1 \geq 0$) highpass IIR butterworth filter (15, 16), to avoid phase distortion and transients (8):

> The transient response and the phase shift are eliminated by treating the FID as though it had mirror symmetry about the first and the final data points. [The signal is here supposed to be discrete.] The filter is run forward over the FID, with a weighting function that increases from zero to one, the output from this stage of the filtering being ignored. With the filter now initialized, the data are filtered from the last point to the first point and the filtered data saved. The frequency-dependent phase shift is then eliminated by running the filter forward from the first to the last data point of the filtered data to give the final output.

When the FID dies away to zero, the first initialization step can be avoided, as we will do in the sequel of this section. In that case, the solvent suppressed signal is

$$S_C(t) = (f * (S''_C + S'_C)(t))U(t) \qquad [29]$$

$$= \langle (\bar{f})_{t,0}, S''_C + S'_C \rangle U(t), \qquad [30]$$

where

$$S'_C(t) = (\bar{f} * S(t))U(t) = \langle f_{t,0}, S \rangle U(t)$$

$$S''_C(t) = \begin{cases} S(-t) & \text{if } t < 0, \\ 0 & \text{otherwise.} \end{cases} \qquad [31]$$

One can show that, if $t > 0$,

$$S'_C(t) = f^* * S''_C(-t).$$

As f is real, the symmetry stated by Cross is respected by this mathematical formulation.

Figure 4 is an unfolded illustration of this scheme. The filter denoted by (b) in the figure implements both the backward filtering and the last forward filtering step: for $t < 0$, the output of this filter is the output of the backward filtering step. It is equal to the input of the filter at point $-t$, which is also the output

of the filter (a) at $-t$. For $t > 0$ the output of the filter (b) is the output of the last forward filtering step. So we conclude that the input of the filter (b) is not continuous. One can expect that this scheme will not totally suppress the solvent peak and might distort the metabolite signals.
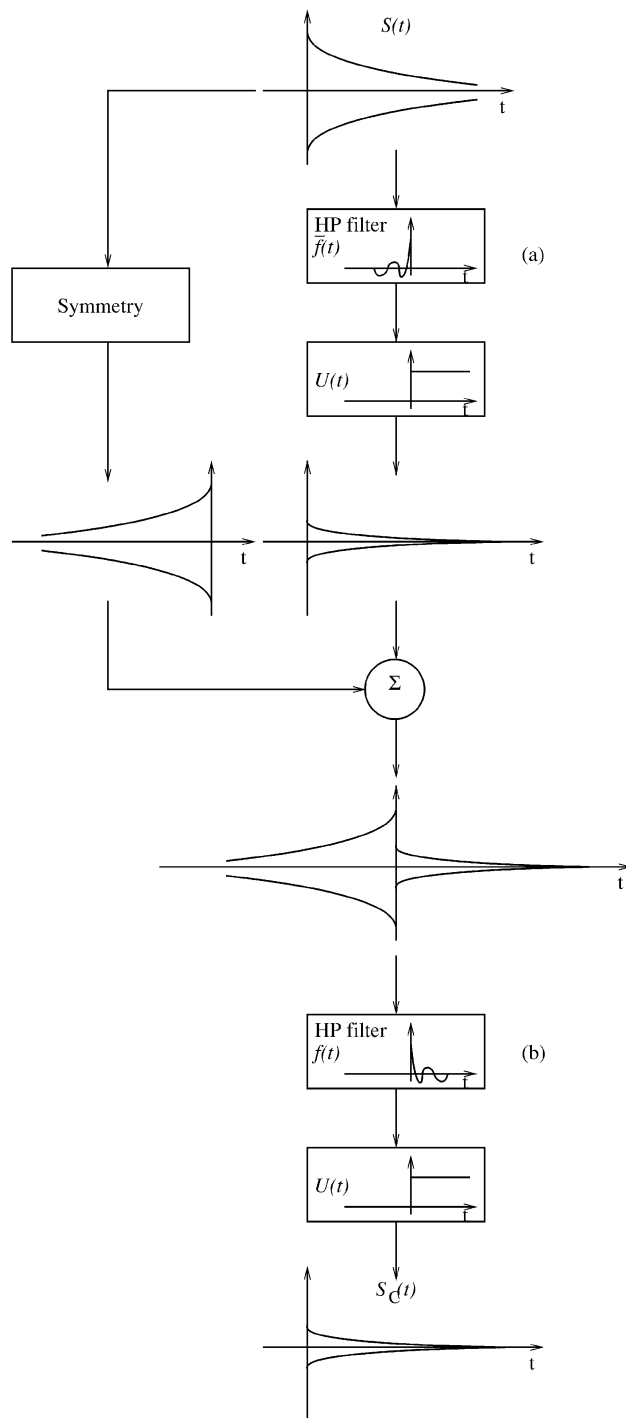

FIG. 4. Schematic representation of the Cross method. The first initialization step is not represented.

If we notice that $\bar{\bar{f}} = f$, an approximate formulation of S_C', with S as [10] on $\mathbb{R}$ is

$$S_C'(t) \approx \left(S_0(t+l)\hat{f}^*(0) + \sum_{k=1}^m S_k(t)F_{f,k}(0) \right)U(t).$$

So a very rough approximation of $S_C(t)$ for large positive t is

$$S_C(t) \approx S_0(t)|\hat{f}(0)|^2 + \sum_{k=1}^m S_k(t)F_{f,k}(0)F_{\bar{f},k}(0)$$

$$\approx S_0(t)|\hat{f}(0)|^2 + \sum_{k=1}^m S_k(t)\int_{\mathbb{R}} \Gamma_f^*(\tau)e^{-d_k\tau}e^{i\omega_k\tau}\,d\tau$$

$$\approx S_0(t)|\hat{f}(0)|^2 + \sum_{k=1}^m S_k(t)F_{\Gamma_f,k}(0) \qquad [32]$$

with Γ_f the autocorrelation of f. However, as f is an IIR filter, $F_{\bar{f},k}(0)$ might be very large or infinite. If the damping d_k is near 0, and $\Gamma_f(\tau)$ decreases quickly, another approximation could be written

$$S_C(t) \approx S_0(t)|\hat{f}(0)|^2 + \sum_{k=1}^m S_k(t)|\hat{f}(\omega_k)|^2. \qquad [33]$$

We have checked that these two filtering steps might avoid phase distortion. But, for small t, the solvent peak may not be suppressed, and the metabolite peaks might be distorted. Hence, we will not propose any parameter correction.

One should also remark that filtering a signal twice with a real filter, once forward and once backward, is equivalent to filtering a signal with a single filter whose impulse response is real and symmetric about 0. This makes the connection with some of the previous methods where a symmetric real FIR filter was used.

2.6. The Maximum Phase Method of Sundin et al.

The signal is filtered with a causal ($T_1 \geq 0$) finite length ($T_2 < \infty$) high pass filter (see Fig. 5). An automatic filter design scheme (9) takes care of the appropriate choice of the filter parameters and estimates the position $\dot{\omega}_0$ of the largest peak in the spectrum. The only parameter the user must specify is the approximate frequency of the peak of interest that lies closest to the water peak. After filtering we get $G_{\bar{f},S}(t, \dot{\omega}_0)$. Points of $G_{\bar{f},S}(t, \dot{\omega}_0)$ whose abscissa are smaller than T_2 are removed. By the use of a maximum-phase filter, the information content lost by discarding those points is minimal. The signal with the solvent peak suppressed can be written as (see Eqs. [6], [7], and [10])

$$S_{Su}(t) = f_{0,\dot{\omega}_0} * S(t) = G_{\bar{f},S}(t, \dot{\omega}_0)$$

$$\approx \left(S_0(t-l)e^{i\omega_0 l}\hat{f}(\omega_0 - \dot{\omega}_0) + \sum_{k=1}^m S_k(t)F_{\bar{f},k}(\dot{\omega}_0) \right)$$
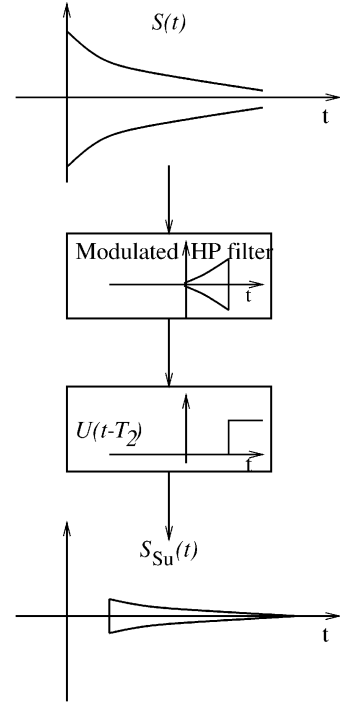
$$\times U(t-T_2). \qquad [34]$$

FIG. 5.   Schematic representation of the Sundin method.

And $0 \leq l \leq T_2$ because the impulse response of the filter is causal, not centered around 0. If we change the origin $\tau = t - T_2$, we obtain

$$S_{Su}(\tau) \approx \left(S_0(\tau + T_2 - l)e^{i\omega_0 l}\hat{f}(\omega_0 - \dot{\omega}_0) \right.$$

$$\left. + \sum_{k=1}^m A_k e^{-d_k T_2}e^{i\omega_k T_2}F_{\bar{f},k}(\dot{\omega}_0)e^{-d_k\tau}e^{i(\omega_k\tau+\phi_k)} \right)U(\tau).$$

$$[35]$$

Compare [11] (respectively, [12]) with [34] (respectively, [35]). If $\hat{f}(\omega_0 - \dot{\omega}_0) = 0$ the solvent and its tail are suppressed. The signal is again a sum of modulated damped exponentials whose parameters can be estimated using any of the standard estimation methods. An estimate of the original parameters can be obtained from A_k', d_k', ω_k', and ϕ_k' using the formulas

$$\dot{A}_k = A_k' \frac{e^{d_k' T_2}}{\left| F_{\bar{f},k}(\dot{\omega}_0) \right|} \qquad [36]$$

$$\dot{d}_k = d_k' \qquad [37]$$

$$\dot{\omega}_k = \omega_k' \qquad [38]$$

$$\dot{\phi}_k = \phi_k' - \omega_k' T_2 - \arg(F_{\bar{f},k}(\dot{\omega}_0)). \qquad [39]$$

However, estimation cannot be performed with standard methods if prior knowledge concerning the amplitudes or

TABLE 1
Summary of the Methods

Property	Gabor	Marion	Sodano	Cross	Sundin
Filter	Lowpass	Lowpass	Lowpass	Highpass	Highpass
Solvent peak position	Anywhere	0 Hz	0 Hz	0 Hz	Anywhere
Automatic filter design	No	No	No	No	Yes
Metabolite distortion	No	Yes	No	Yes	No

phases is to be taken into account. The influence of the filter on these parameters must be considered directly in the estimation procedure to yield correct estimates. In (9) it is proposed to minimize the squared difference between the filtered signal and the filtered model function derived in Eq. [35]. The quantitation method taking into account the influence of the filter in the minimization procedure is denoted by AMARES$_f$.

2.7. Summary

We summarize in Table 1 the main characteristics of the different methods. In the row "Metabolite distortion" a "Yes" means that the filtered metabolite signals are no longer damped exponentials. With the Marion method, this distortion is limited to the first points. The row "Solvent peak position" describes the position of the solvent peak when applying Eq. [1]. If the signal is complex and the water peak is not at 0 Hz, Marion, Sodano, and Cross methods can be applied after shifting the water peak to zero by modulation. The other methods prefer modulating the filter.

All the methods assume that the solvent peak is regular enough to be suppressed by filtering. However, because of the discontinuity at 0, one cannot recover easily the first points. Marion *et al.* extrapolate those points, Cross tries to enhance the regularity of the signal, Sodano and Delepierre subtract a translated version of the extracted peak, and Sundin *et al.* discard the first points but use a maximum-phase filter to minimize the information lost in these samples.

From a quantitative perspective, properly recovering those first points is important because the power of the signal is maximum here. However, if it is not possible, dropping them could be a better solution.

One should remark that the preceding methods are based on filtering and some other treatments like the multiplication of a filtered signal by $U(t)$. The solvent suppressed signal *cannot* be written as a single convolution of the FID with a function f, because of the latter operation. As a consequence the Fourier transform of the solvent suppressed signal *cannot* be written as a single product of the Fourier transform of the FID and f.

If the metabolite component is not a Lorentzian and varies quickly, then the model function of the metabolite is altered by filtering for $t < T_2$ *and* for $t \geq T_2$. The shape of the metabolite signal S_k after filtering is changed to S'_k. To quantify the original

metabolite signal, one has to fit the metabolite signal after filtering with S'_k and map those extracted parameters to the original parameters of S_k. In summary, if the appropriate model function of the metabolites is known, a similar derivation as was done in Eqs. [13]–[16] can be made to investigate the effect of the filter on the model function of the metabolites.

3. THE TEST EXAMPLE

Our test example simulates a ^{1}H MRS signal. Experimental ^{1}H signals are normally acquired with some water suppression technique, however some water signal usually remains. Each simulated signal of our dataset is the sum of three components: residual water, five metabolites, and noise. The amplitude ratios between residual water and metabolite peaks are usually between 10 and 100, and the linewidths of the metabolite peaks are typically between 5 and 12 Hz.

The simulated signal was derived from an experimental signal obtained from a water solution of 100 mM creatine (Cr) (CH$_2$ singlet, peak 1; CH$_3$ singlet, peak 2), 100 mM acetate (CH$_3$ singlet, peak 3), 50 mM t-butyl alcohol (3 × CH$_3$ singlet, peak 4), and 10 mM trimethylsilylpropionic acid (TSP, 3 × CH$_3$ singlet, peak 5). A single-voxel signal from a spherical phantom was acquired at 1.5 T (Vision, Siemens) using the STEAM sequence (TR/TE/TM = 20000/20/30 ms) with selective water suppression. The acquired phantom signal was quantified with HSVD using a high model order ($M = 100$). The residual water signal was subsequently reconstructed with all the exponentially damped sinusoids with frequencies between [−30 and 30] Hz and with amplitudes above the estimated noise level $\hat{\sigma} \simeq 7.5$. The parameters of the seven peaks used to reconstruct the water resonance are found in Table 2.

The five metabolite peaks were modeled as exponentially damped sinusoids with frequency, phase, and damping close to what was measured in the phantom experiment. The amplitudes of the peaks were chosen to be approximately equal to the estimated TSP amplitude and set equal for all peaks except for the two Cr peaks whose 2 : 3 ratio was kept. The signals (FIDs) are 512 points long with a sampling frequency of 1000 Hz. The exact parameters used in the simulation examples are given in Table 3. The amplitude ratio between the residual water peak

TABLE 2
Estimated Water Signal Parameters Used in the Reconstruction of the Water Peak

f_{w_k} (Hz)	d_{w_k} (Hz)	ϕ_{w_k} (°)	A_{w_k} (a.u.)
−8.48	5.10	−90.88	15.01
−5.25	8.28	−45.19	64.74
−2.16	10.51	−2.95	321.25
−0.18	12.45	179.97	1142.30
−0.17	4.24	−170.39	251.92
3.09	6.79	36.77	201.11
6.31	4.00	81.11	12.30

CORON ET AL.

TABLE 3
Metabolite Parameters Used in the Simulated Signals

| Peak k	f_k (Hz)	d_k (Hz)	ϕ_k (°)	A_k (a.u.)
1	61	7	0	20
2	118	7	0	30
3	189	7	0	20
4	231	7	0	20
5	311	7	0	20

(frequency around 0) and the closest metabolite peak (peak 1, frequency 61 Hz) is 43.

The added complex noise was white and circular Gaussian distributed. The noise standard deviation was varied to simulate seven SNR. The standard deviation of the real or imaginary part of the circular Gaussian white noise was equal to $\sigma_k = 20 \times 10^{(-35+5k)/20}$ with $k \in \{1, \ldots, 7\}$. 400 signals with different noise realizations were simulated for each of the 7 noise levels. The modulus of the Fourier transform of one signal of the dataset is plotted in Fig. 6.

3.1. Visual Inspection

The description of the Gabor, Marion *et al.*, and Sodano and Delepierre methods does not impose a finite length filter but let the user choose one. Our test window is the common Hamming window (*17*) of length $2T_2 + 1$:

$$f(k) = \begin{cases} 0.54 + 0.46\cos(\pi k/T_2) & |k| \leq T_2 \\ 0 & \text{otherwise.} \end{cases}$$
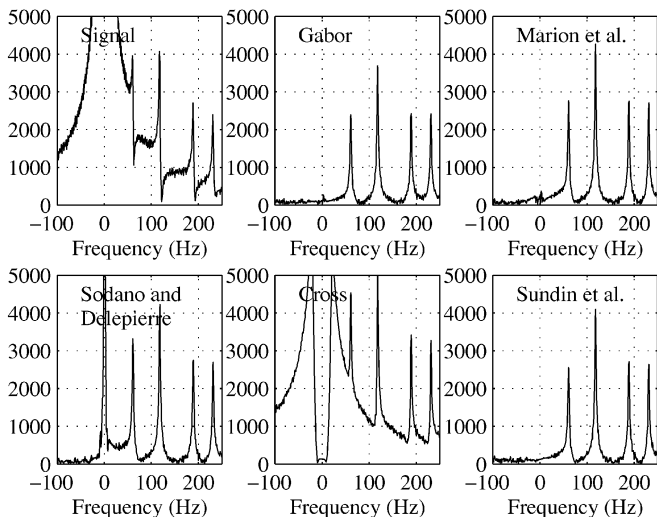
FIG. 6. Example of spectra magnitude before and after removing the residual water signal with the different methods. Noise level 3, Method parameters: *Gabor:* 35 points Hamming window; *Marion et al.:* 45 points Hamming window, $M = 44$; *Sodano and Delepierre:* 21 points Hamming window; *Cross:* 6 order Butterworth filter, cuttoff frequency 20 Hz.
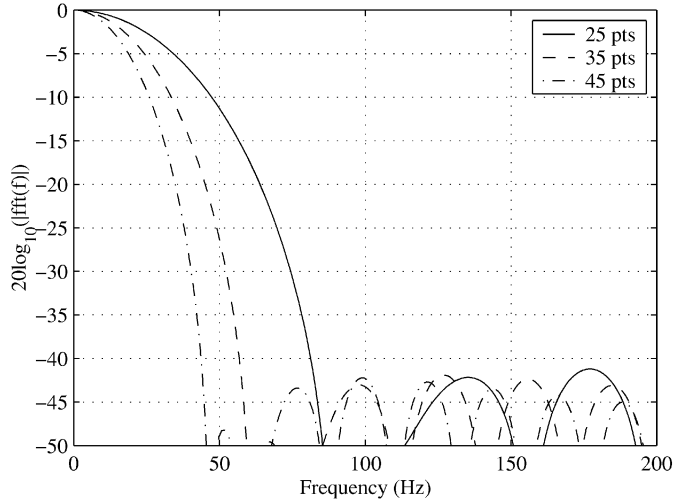
FIG. 7. Magnitude of the Fourier Transform of Hamming windows of different length.

The window is normalized such that $\sum_k f(k) = 1$. Its highest sidelobe is at -43 dB which is -20 dB lower than the highest sidelobe of a sine-shaped function. Its spectrum is plotted in Fig. 7 for different lengths. The width of the main lobe decreases when the length of the window increases. A 25 points window is -17.9 dB at 0.061 Hz and is probably not long enough for separating the water peak from the first metabolite peak.

As recommended (*8*), we use a sixth order Butterworth filter with different bandstop widths in the Cross case.

We now control the efficiency/effect of the methods by visual inspection of the spectra after water filtering. Parameters indicated in Fig. 6 were chosen because our subsequent statistical analysis demonstrates their relevance. The water peak is well suppressed with methods of Gabor, Marion *et al.*, and Sundin *et al.*, but not with the schemes of Cross or Sodano and Delepierre. With Sodano, an attenuated water peak remains because the term $S_0(t) - S_0(t+T_2)\hat{f}(0)$ in Eq. [24] cannot be neglected. In other words, the water peak is not stationary enough on the filter length. The Cross method does not suppress the tails of the water peak.

3.2. Statistical Inspection

The previous inspection is not sufficient, and we will check whether:

• the metabolite parameters can be estimated without bias after water peak suppression,
• the root mean square errors of the estimated parameters are close to the Cramér–Rao Bounds (CRB) of the standard deviations for unbiased estimators,
• our proposed parameter corrections are relevant.

Quantitation is performed with the model fitting method AMARES. When testing the method of Sundin *et al.*, quantitation is also performed with AMARES$_f$, a nonlinear
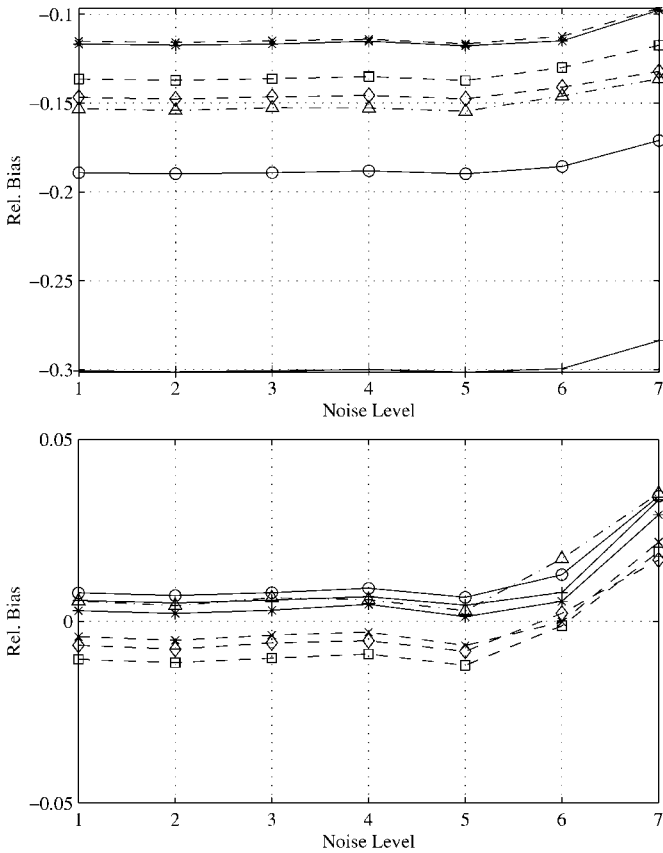
FIG. 8. Estimated relative amplitude bias with Gabor method. (Top) No correction applied; (Bottom) Correction applied. Each mark corresponds to a specific window length: (+) 21 points, (○) 25 points, (∗) 31 points, (×) 35 points, (□) 41 points, (◇) 45 points, (△) 51 points.

least squares algorithm which takes into account the filter effect.

The parameters, amplitude, frequency, damping, and phase are estimated without any prior knowledge.

To shorten the study, we will only focus on the quality of the amplitude of peak 1 at 61 Hz. This peak stands very close to the water peak and is therefore more affected by the treatment than the others.

3.2.1. Which methods are unbiased?. In Figs. 8 to 12 we plot the relative amplitude bias for each method. We would like to stress that:

• After a Gabor removal scheme, the quantification is biased. But the proposed correction leads to unbiased estimates. It is robust in the sense that unbiased results are obtained, except at noise level 7 (lowest SNR), with all the tested windows, so even if the mainlobe of the filter spectrum overlaps with the metabolite peak.

• The amplitude quantification after Marion *et al.* removal is unbiased only if the metabolites are in the stopband region of the filter (window length ≥31 points). The proposed correction is not efficient.

• Generally speaking the amplitudes are slightly over-estimated after Sodano and Delepierre removal, except with the 31 points window. Results obtained with a 21 points window are out of the axis limits. The proposed corrections are necessary especially when the window is short, but the estimated amplitude is still slightly biased. A short examination on peak 2, confirms this conclusion and it is supported by the fact that the water peak is not totally suppressed.

• In many cases the quantification algorithm does not converge after the Cross removal method. When it converges, the result is biased.
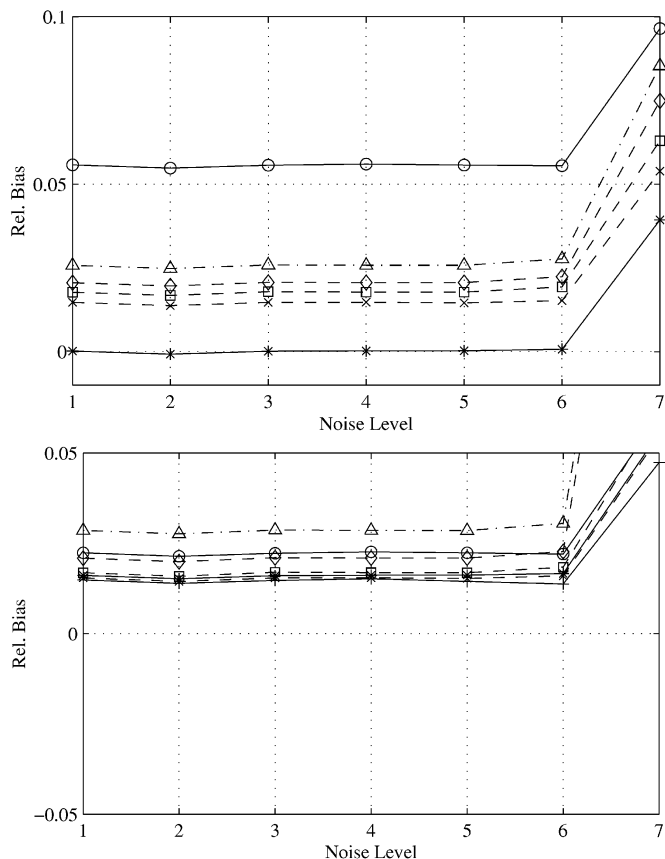
• If the signal is filtered with the maximum phase filter and then quantified with AMARES, a bias exists. To avoid bias, one can correct those estimates *a posteriori* as in Eqs. [36] to [39] or, as explained in Section 2.6 one can use AMARES$_f$, which includes the effect of the filter in the quantitation algorithm. Both methods are as efficient at high SNR, but the latter seems slightly better at low SNR.

• At noise level 7, all methods are slightly biased.

3.2.2. Root mean square error. The Cramér–Rao bound (CRB) is equal to the lowest variance/standard deviation that
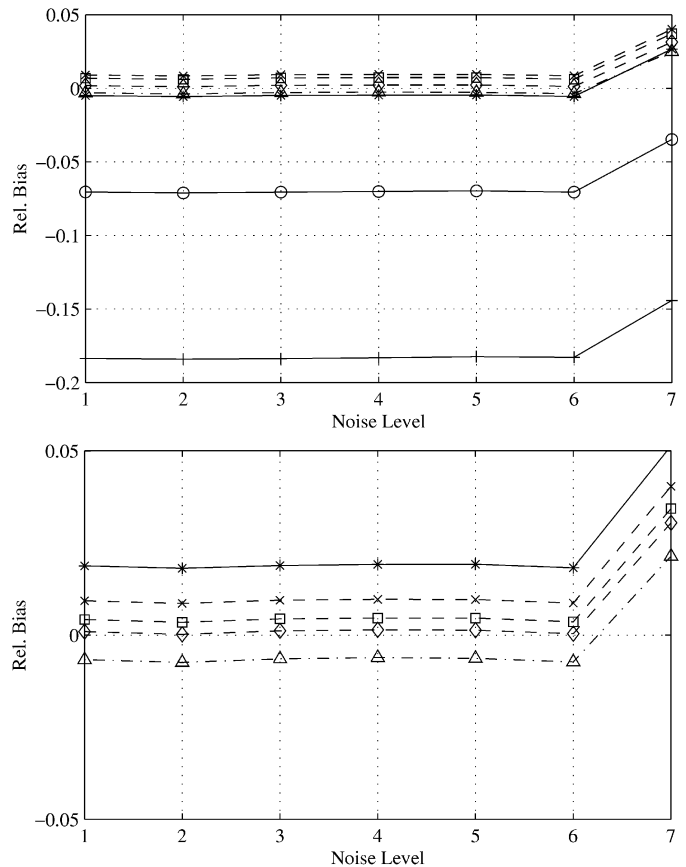
FIG. 9. Estimated relative amplitude bias with the method of Marion *et al.* (Top) No correction applied; (Bottom) correction applied. Each mark corresponds to a specific window length: (+) 21 points, (○) 25 points, (∗) 31 points, (×) 35 points, (□) 41 points, (◇) 45 points, (△) 51 points. M is equal to the length of the window minus 1.
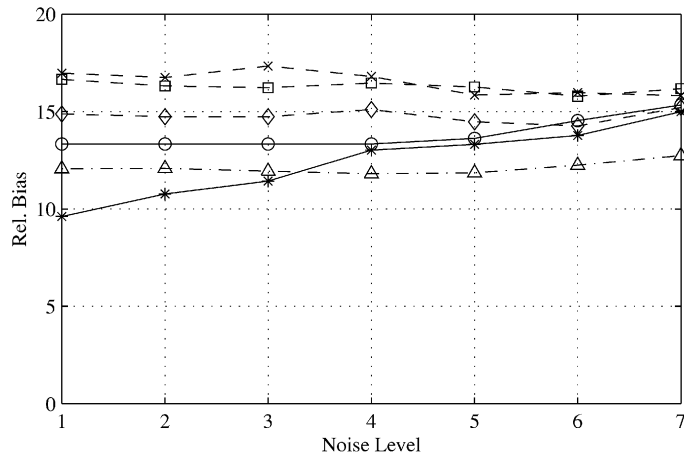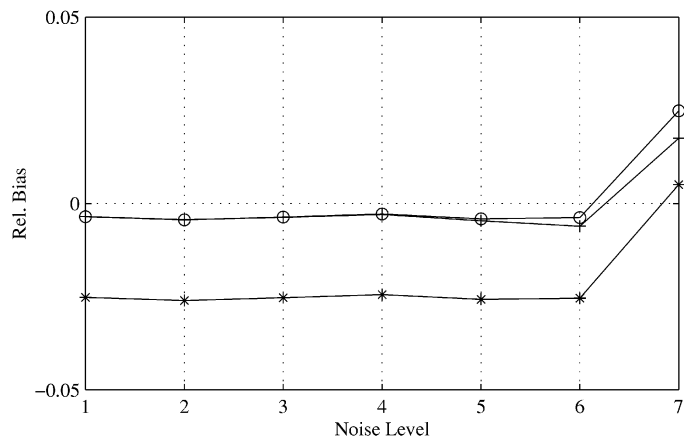
FIG. 11. Estimated relative amplitude bias with the method of Cross: no correction applied. Each mark corresponds to a specific cutoff frequency of the 6th order highpass filter measured at −3 dB: (+) 15 Hz, (○)20 Hz, (∗) 25 Hz, (×) 30 Hz, (□) 35 Hz, (◇) 40 Hz, (△) 45 Hz.

FIG. 10. Estimated relative amplitude bias with the method of Sodano and Delepierre. (Top) No correction applied; (Bottom) correction applied. Each mark corresponds to a specific window length: (+) 21 points, (○) 25 points, (∗) 31 points, (×) 35 points, (□) 41 points, (◇) 45 points, (△) 51 points.

one can expect from an unbiased estimator. This bound increases with the noise level (*18*). However, we are not interested in its fluctuations, but in the relation between the Root Mean Square Error (RMSE) of the estimator and the lowest standard deviation over all sets of unbiased estimators. So we will plot the quantity RMSE/CRB$_\sigma$.

The previous quantity is only meaningful for an unbiased estimator. So, the following will concern:

- the corrected parameter estimates after Gabor solvent removal,
- the noncorrected parameter estimates after Marion *et al.*, solvent removal,
- the corrected parameter estimates after Sodano and Delepierre solvent removal
- the parameters estimated with AMARES$_f$, or the *a posteriori* corrected parameter estimates after maximum phase filtering.

As the Cross method leads to highly biased results, we exclude it from this analysis.

In Figs. 13 to 16 we focus on the amplitude. According to these results one observes that:

- The performance of the Gabor method is close to the theoretical lower bound provided one chooses the window length correctly. Short windows are preferred because long windows, although they properly separate the water peak and the metabolites, require the removal of a large number of points at the beginning of the treated signal, resulting in a degradation of the quality of the parameter estimates due to an increase in standard deviation.
- The performance of the method of Marion *et al.* may be good at low or high SNR as long as the window is longer than 35 points. A correct window length choice is crucial to avoid inaccurate estimates.
- At high SNR, the RMSE with the solution of Sodano and Delepierre is far from the CRB and one cannot recommend this

FIG. 12. Estimated relative amplitude bias when using a maximum phase filter to suppress the solvent peak. The filter is chosen according to Sundin *et al.* (*9*): (∗) the FID is filtered and then quantified with AMARES; (○) the FID is filtered, quantified with AMARES, and the estimates are corrected *a posteriori* (see Eq. [36]); (+) AMARES$_f$.
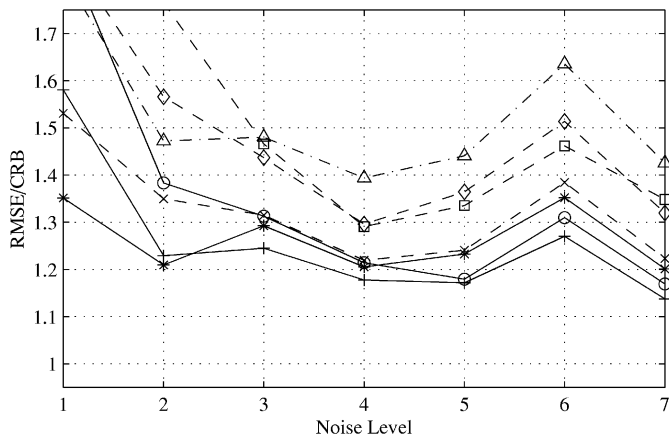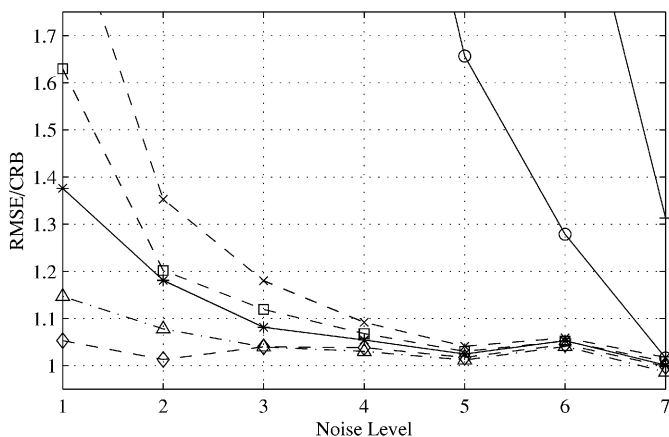
FIG. 13. Ratio of the RMSE to the Cramér–Rao bound of the amplitude with Gabor method. The estimated parameters were corrected. Each mark corresponds to a specific window length: (+) 21 points, (○) 25 points, (∗) 31 points, (×) 35 points, (□) 41 points, (◇) 45 points, (△) 51 points.
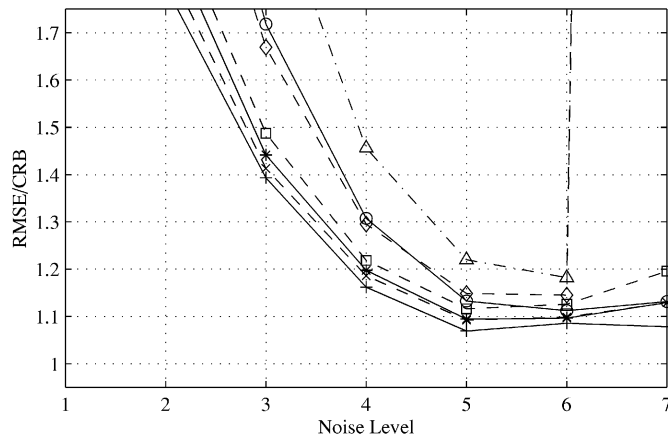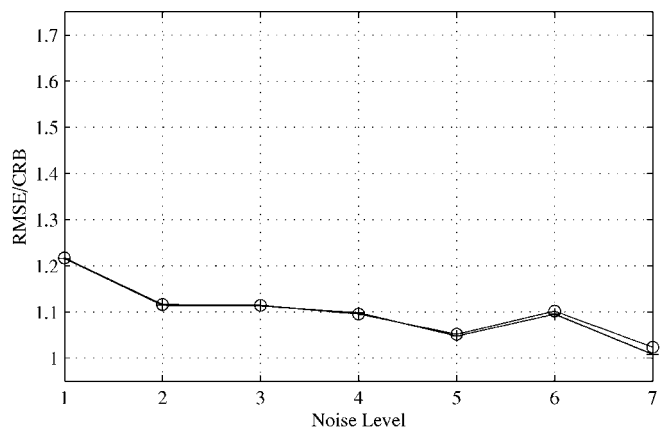

FIG. 15. Ratio of the RMSE to the Cramér–Rao bound of the amplitude with the method of Sadano and Delepierre and with parameter correction. Each mark corresponds to a specific window length: (+) 21 points, (○) 25 points, (∗) 31 points, (×) 35 points, (□) 41 points, (◇) 45 points, (△) 51 points.

method. At noise level 5, it seems better. Is a short window preferable to a long window? This is not obvious, since two effects compete against each other. A short filter implies a short translation of the extracted solvent component and also a filter with a large transition band. So, those filters are not very selective. To reduce the transition band, longer filters can be chosen, but the length of the translations involved in the method of Sodano and Delepierre increases.

• Filtering with a maximum phase filter and then quantifying the signal leads to very satisfactory results. A slight advantage is gained from taking into account the filter correction in the quantification step as proposed by Sundin *et al.* (and not *a posteriori*).

3.2.3. Discussion. As suspected, the Cross method did not lead to reliable quantification. When preparing this publication,

we have investigated various variations, like executing the whole filtering step in the reverse direction: The initialization step is driven backward, then we filter forward and then backward. From a theoretical perspective, this is equivalent to filter a more regular signal. However, quantification results were not as good as those obtained with the method of Sundin *et al.*

In our experiment, the scheme of Sodano and Delepierre does not remove totally the water signal. The estimated damping (not plotted) is biased. The estimated amplitude is also biased, especially with a short window. In that case, correcting this parameter is essential. But, in our example, a bias remains even with corrected parameters. It seems difficult to choose a window length for which quantification will surely perform well, especially at high SNR.

The Gabor method leads to biased estimates of the amplitude and unbiased estimates of the damping (not plotted). Correcting

FIG. 14. Ratio of the RMSE to the Cramér–Rao bound of the amplitude with the method of Marion *et al.* and without parameter correction. Each mark corresponds to a specific window length: (+) 21 points, (○) 25 points, (∗) 31 points, (×) 35 points, (□) 41 points, (◇) 45 points, (△) 51 points. M is equal to the length of the window minus 1.

FIG. 16. Ratio of the RMSE to the Cramér–Rao bound of the amplitude when using a maximum phase filter to suppress the solvent peak. The filter is chosen according to (9): (○) the FID is filtered, quantified with AMARES, and the estimates are corrected *a posteriori* (see Eq. [36]); (+) AMARES$_f$.

the amplitude parameter is essential and leads to an unbiased estimator. This method is not very sensitive to the choice of a window. However the variance of the estimated parameter is rather large at low or high SNR.

The method of Marion *et al.* sometimes outperforms all the other methods, but it may also be very unsatisfactory at high SNR. For example, we have noticed that the ratio RMSE/CRB$_\sigma$ of the amplitude of peak 3 is equal to 1.75 with the same 45 points Hamming window which quantifies very well peak 1. A correct choice of M is also critical and difficult. At low SNR this method may be recommended and is less sensitive to the chosen parameters than at high SNR.

Filtering with a maximum phase filter and quantifying the remaining signal leads to overall excellent results when taking into account the filter effects. The estimated parameters are unbiased and RMSE/CRB$_\sigma$ is always lower than 1.25. Sundin *et al.* proposed to take into account the filter correction during quantification. The slight advantage over *a posteriori* correction is confirmed when analysing the other peaks. Furthermore, if prior knowledge is available, the method of Sundin *et al.* can take it into account.

4. CONCLUSION

Many spectral line removal techniques are based on the filtering concept. From a signal processing perspective, they mainly differ on the treatment of the first FID points.

Furthermore this study emphasizes two key points:

• FID quantification must take into account the spectral line removal processing if one intends to estimate the metabolites concentration without bias and with high accuracy. This conclusion is very general and future quantification techniques must include corrections based on all the acquisition steps. They cannot be independent from the acquisition technique.

• Among the five post-processing methods tested, the most efficient method in terms of quantification after spectral line removal is the one proposed by Sundin *et al.* (*9*). It has several advantages:

—it is the only one that is fully automatic —even if most of the other methods could be automated.

—it is unbiased and its performances are very close to the best possible method at high or low SNR for the damping and the amplitude. The maximum phase filter better takes into account the information contained in the first point of the FID and yet does not need additional assumptions on the solvent signal.

—prior knowledge may be taken into account during quantitation.

So Sundin's method should be considered as the reference method for spectral line removal based on FID filtering.

With spin-echo sequences there is no border effect and the problem is slighty different. A filter based method should remove very well the solvent line. As in the FID case, the quantification

step should include some correction terms which depends on the chosen filter.

APPENDIX A

Some Basic Properties of the Fourier Transform

We consider signals of finite energy, $f \in L^2(\mathbb{R})$. The Fourier transform of f is denoted by $\hat{f}$, namely,

$$\hat{f}(\omega) = \int_{\mathbb{R}} f(t)e^{-i\omega t}\, dt \qquad [40]$$

The signal f can be recovered from its Fourier transform $\hat{f}$ by the inversion formula:

$$f(t) = \frac{1}{2\pi} \int_{\mathbb{R}} \hat{f}(\omega)e^{i\omega t}\, d\omega. \qquad [41]$$

With $p \in \mathbb{N}$ and $g(t) = (-it)^p f(t)$ in $L^2(\mathbb{R})$, the pth derivative of $\hat{f}$ is equal to the Fourier transform of g:

$$\hat{f}^{(p)}(\omega) = \hat{g}(\omega). \qquad [42]$$

One can prove that if

$$\int_{\mathbb{R}} |\hat{f}(\omega)|(1 + |\omega|^p)\, d\omega < +\infty, \qquad [43]$$

the function f is bounded and p times continuously differentiable with bounded derivatives. The decay of $|\hat{f}|$ at high frequencies depends on the worst singular behaviour of f. So, if f is discontinuous at one point (and continuous everywhere else), $|\hat{f}(\omega)|$ decreases slowly, typically like $\frac{1}{|\omega|}$. So the spectrum is largely affected by this local discontinuity or this local worst behavior.

Another well-known property is the convolution theorem. Suppose that f and g are in $L^2(\mathbb{R})$, then the convolution product $h(t)$,

$$h(t) = f * g(t) = \int_{\mathbb{R}} f(t - \tau)g(\tau)\, d\tau \qquad [44]$$

is *continuous*. In terms of Fourier transform one has

$$\hat{h}(\omega) = \hat{f}(\omega)\hat{g}(\omega). \qquad [45]$$

APPENDIX B

Approximate Expression of the Gabor Transform of a Water or Metabolite Peak

We seek an approximate expression of $G_{\bar{f},S}(t, \omega)$. S is supposed to be a water or metabolite peak whose definition is given at the beginning of Section 2.1.

Most of the following results and approximations come from the time-frequency/scale analysis (2, 4, 19).

We say that a function A is regular on an interval $I = [a, b]$, if for some $n \in \mathbb{N} \backslash \{0\}$, $A^{(n-1)}(\tau)$, the $n-1$ derivative of A, is continuous on $[a, b]$ and $A^{(n)}(\tau)$ exists for every $\tau \in (a, b)$.

Under the assumption that $U(\tau)A(\tau)$ is regular enough on $I_t = [-T_2 + t, -T_1 + t]$ (so $t \notin [T_1, T_2)$), Taylor's theorem implies that, for every α and β in I_t, there exists a point x between α and β such that

$$U(\beta)A(\beta) = \sum_{k=0}^{n-1} \frac{A^{(k)}(\alpha)}{k!}(\beta - \alpha)^k + \frac{A^{(n)}(x)}{n!}(\beta - \alpha)^n \quad [46]$$

$$= \sum_{k=0}^{n-1} \frac{A^{(k)}(\alpha)}{k!}(\beta - \alpha)^k + r_{n,\alpha}(\beta)(\beta - \alpha)^n. \quad [47]$$

If $|A^{(n)}(\tau)|$ is bounded, $r_{n,\alpha}(\beta)$ will also be bounded

$$|r_{n,\alpha}(\beta)| \leq \frac{1}{n!} \sup_{\tau \in (-T_2+t, -T_1+t)} |A^{(n)}(\tau)|.$$

Let l be the point where f is maximum or the average location. In the latter case,

$$l = \frac{\int_{\mathbb{R}} t |f(t)|^2 \, dt}{\int_{\mathbb{R}} |f(t)|^2 \, dt}.$$

We rewrite Eq. [1] expanding $A(t)$ around $t - l$, with the additional hypothesis: $t \geq T_2$, which means that we are seeking for an approximation outside of the transients. Then,

$$G_{\bar{f},S}(t, \omega) = \int_{T_1-l}^{T_2-l} f(v + l) e^{i\omega(v+l)} S((t-l) - v) \, dv$$

$$= e^{i(\omega_0(t-l)+\phi+\omega l)} \int_{T_1-l}^{T_2-l} f(v+l) A((t-l) - v)$$

$$\times e^{i(\omega - \omega_0)v} \, dv$$

$$= e^{i(\omega_0(t-l)+\phi+\omega l)}$$

$$\times \left[\sum_{j=0}^{n-1} \frac{A^{(j)}(t-l)}{j!} \int_{T_1-l}^{T_2-l} f(v+l)(-v)^j \right.$$

$$\times e^{-i(\omega_0 - \omega)v} \, dv + \int_{T_1-l}^{T_2-l} f(v+l)(-v)^n$$

$$\left. \times r_{n,t-l}((t-l) - v) e^{-i(\omega_0 - \omega)v} \, dv \right]. \quad [48]$$

With Eq. [42], the first n terms in square brackets of Eq. [48] may be rewritten as

$$B_j(t, \omega) = \frac{1}{j!} A^{(j)}(t-l)(-i)^j \widehat{f_{-l,0}}^{(j)}(\omega_0 - \omega),$$

$$j = 0, \ldots, n-1.$$

The last term may be bounded,

$$|C_n(t, \omega)| = \left| \int_{T_1-l}^{T_2-l} f(v+l)(-v)^n r_{n,t-l}((t-l) - v) \right.$$

$$\left. \times e^{-i(\omega_0 - \omega)v} \, dv \right|$$

$$\leq \frac{\sup_{\tau \in (-T_2+t, -T_1+t)} |A^{(n)}(\tau)|}{n!}$$

$$\times \int_{T_1-l}^{T_2-l} |f(v+l)||v|^n \, dv,$$

for instance if the impulse response of the filter f is finite. This bound essentially depends on the supremum of $|A^{(n)}(\tau)|$ on $(-T_2 + t, -T_1 + t)$.

In particular, with $n = 1$,

$$G_{\bar{f},S}(t, \omega) = e^{i(\omega_0(t-l)+\phi+\omega l)}(A(t-l) \widehat{f_{-l,0}}(\omega_0 - \omega) + C_1(t, \omega))$$
$$[49]$$

$$= S(t-l) e^{i\omega_0 l} \hat{f}(\omega_0 - \omega) + e^{i(\omega_0(t-l)+\phi+\omega l)} C_1(t, \omega)$$
$$[50]$$

Then, under the assumption that $A(\tau)$ varies slowly on $[-T_2 + t, -T_1 + t]$, which means that $A^{(1)}(\tau)$ is very small on this interval, $G_{\bar{f},S}(t, \omega_0)$ and the filtering method lead to good approximations of S up to a correction term.

ACKNOWLEDGMENTS

REFERENCES

1. W. S. Price, Water signal suppression in NMR spectroscopy, *Annu. Rep. NMR Spectrosc.* **38**, 289–354 (1999).

2. J.-P. Antoine, A. Coron, and J.-M. Dereppe, Water peak suppression: Time-frequency vs time-scale approach, *J. Magn. Reson.* **144**(2), 189–194 (2000).

3. D. Barache, J.-P. Antoine, and J.-M. Dereppe, The continuous wavelet transform, an analysis tool for NMR spectroscopy, *J. Magn. Reson.* **128**(1), 1–11 (1997).

4. N. Delprat, B. Escudié, P. Guillemain, R. Kronland-Martinet, P. Tchamitchian, and B. Torrésani, Asymptotic wavelet and Gabor analysis: Extraction of instantaneous frequencies, *IEEE Trans. Inform. Theory* **38**(2), 644–664 (1992).

5. P. Guillemain, R. Kronland-Martinet, and B. Martens, Estimation of spectral lines with the help of the wavelet transform—Application in N.M.R. spectroscopy. *in* "Wavelets and Applications—Proceedings of the International Conference Marseille, France, May 1989" (Y. Meyer, Ed.), pp. 38–60. Éditions Masson, Paris and Springer-Verlag, Berlin, 1991.

6. D. Marion, M. Ikura, and A. Bax, Improved solvent suppression in one- and two-dimensional NMR spectra by convolution of time-domain data, *J. Magn. Reson.* **84**(2), 425–430 (1989).

7. P. Sodano and M. Delepierre, Clean and efficient suppression of the water signal in multidimension NMR spectra, *J. Magn. Reson. Ser. A* **104,** 88–92 (1993).

8. K. J. Cross, Improved digital filtering technique for solvent suppression, *J. Magn. Reson. Ser. A* **101**(2), 220–224 (1993).

9. T. Sundin, L. Vanhamme, P. Van Hecke, I. Dologlou, and S. Van Huffel, Accurate quantification of ^{1}H spectra: From finite impulse response filter design for solvent suppression to parameter estimation, *J. Magn. Reson.* **139**(2), 189–204 (1999).

10. H. G. Feichtinger and T. Strohmer (Eds.), "Gabor Analysis and Algorithms—Theory and Applications." Birkhäuser, Boston, 1998.

11. R. Kumaresan and D. W. Tufts, Estimating the parameters of exponentially damped sinusoids and pole-zero modeling in noise, *IEEE Trans. Acoust. Speech Signal Process.* **30**(6), 833–840 (1982).

12. H. Barkhuijsen, R. de Beer, and D. van Ormondt, Improved algorithm for noniterative time-domain model fitting to exponentially damped magnetic resonance signals, *J. Magn. Reson.* **73,** 553–557 (1987).

13. J. W. C. van der Veen, R. de Beer, P. R. Luyten, and D. van Ormondt, Accurate quantification of *in vivo* ^{31}P NMR signals using the variable projection method and prior knowledge, *Magn. Reson. Med.* **6,** 92–98 (1988).

14. L. Vanhamme, A. van den Boogaart, and S. Van Huffel, Improved method for accurate and efficient quantification of MRS data with use of prior knowledge, *J. Magn. Reson.* **129,** 35–43 (1997).

15. T. W. Parks and C. S. Burrus, "Digital Filter Design." Wiley, New York, 1987.

16. A. V. Oppenheim, R. W. Schafer, and J. R. Buck, "Discrete-Time Signal Processing," Prentice Hall Signal Processing Series, 2nd ed. Prentice Hall International, Englewood Cliffs, NJ, 1999.

17. F. J. Harris, On the use of windows for harmonic analysis with the discrete Fourier transform, *Proc. IEEE* **66**(1), 51–83 (1978).

18. S. Cavassila, S. Deval, C. Huegen, D. van Ormondt, and D. Graveron-Demilly, Cramér–Rao bound expressions for parametric estimation of overlapping peaks: Influence of prior knowledge, *J. Magn. Reson.* **143,** 311–320 (2000).

19. B. Torrésani, "Analyse continue par ondelettes," Savoirs actuels. Inter-Éditions/CNRS Éditions, Paris, 1995.